CHEMICAL ENGINEERING TRANSACTIONS
VOL. 61, 2017
A publication of AIDIC
The Italian Association of Chemical Engineering
Online at www.aidic.it/cet
Guest Editors: Petar S Varbanov, Rongxin Su, Hon Loong Lam, Xia Liu, Jiří J Klemeš

ISBN 978-88-95608-51-8; **ISSN** 2283-9216
DOI: 10.3303/CET1761167

Influence of Defects on Flow and Mass Transfer in The Channel With Micro-Fluidic Chips

Long Li[a], Xiaohong Yan[b], Jian Yang[a], Qiuwang Wang[a,*]

[a]Key Laboratory of Thermo-Fluid Science and Engineering, Ministry of Education, School of Energy and Power Engineering Xi'an Jiaotong University, Xi'an, Shaanxi 710049, P.R. China
[b]Department of Chemical Engineering, Xi'an Jiaotong University, Xi'an, Shaanxi 710049, P.R. China
wangqw@mail.xjtu.edu.cn

Microfabricated pillar arrays are a new type of chromatographic columns, which can improve the performance of separation. However, because microstructure fabrication concerns many problems such as multi-scale flow, heat transfer and so on, the quality control of microstructure is quite complicated. Therefore, there is certain difference of structure parameters between design and actual till now. In the study, the effect of vacancy, damage and dimensional accuracy on flow and mass transfer is discussed. The volume averaging method is applied by the software COMSOL. Vacancy in pillar arrays can increase the reduced plate height significantly. When some micropillars are damaged, the corresponding influence on mass transfer in pillar arrays depends on the size of the missing part. When the arch height of the missing part is less than 30 % of the original diameter, the difference can be ignored. The effect could be neglected when the pillar size fluctuates within the small range. The present results would be useful for the process optimization and the design of high efficiency microstructure.

1. Introduction

Nowadays, microfabrication is used in a wide variety of energy and chemical process industries. For example, Zhu et al. (2017) used solar air collectors with many micro-fins, micro-channels and micro-grooves to enhance the heat transfer. Santana et al. (2015) investigated the mixing performance of the spiral microchannels, and Rahim et al. (2017) focused on the design and optimization of microstructure. Much attention has been devoted to the microstructure. In analytical chemistry, theoretical research and experimental data indicate that the performance in microfabricated pillars is significantly better than that in packed bed columns. Although many sophisticated techniques (Seeger and Palmer, 1999) can be used to control the parameters of the arrays to a certain degree, a precise control over the periodicity, the height of the pillars and their aspect ratio remains a challenge (Sinitskii et al., 2007). Wang et al. (2013) find that the bonded and bent nanopillars can be observed after etching. Fee et al. (2014) demonstrate the use of 3D printing to create porous media, but the difference of structural parameters between the computer aided design (CAD) models and printed models is greater than 1 %. Yan et al. (2015) investigated the hydrodynamic dispersion in rectangular microchannels. In their research, it is expected to fabricate ideal rectangular channels. Nevertheless, the cross-sectional shape is similar to the "T-shape". Therefore, the differences between the design parameters and real parameters are ubiquitous. Much work has been carried out on the improvement of the processing technology to obtain as close replications of idea models as possible. However, the influence of the differences has seldom been discussed, and the connection between the differences and performance change is not clear. In this paper, the effect of the defects from fabrication processing on separation performance is systematically investigated.

2. Volume-averaging equations

In this section, the method of volume-averaging will be employed to describe separation performance of pillars with a thin uniform stationary phase coated on the pillar surface for the retention capacity (Buyuktas and

Please cite this article as: Li L., Yan X., Yang J., Wang Q., 2017, Influence of defects on flow and mass transfer in the channel with micro-fluidic chips, Chemical Engineering Transactions, 61, 1015-1020 DOI:10.3303/CET1761167

Wallender, 2004). The liquid mobile phase is driven by pressure. It is assumed that the medium is homogeneous (Yan et al., 2010). The mobile phase is governed by the Stokes equation:

$$\nabla p = \mu \nabla^2 \mathbf{V} \tag{1}$$

where p, μ and **v** are the pressure, viscosity and velocity.
In general, we consider that the molecular diffusion coefficient is constant. The concentration of the analyte C_m is calculated by solving the advection-diffusion equation (Buyuktas and Wallender, 2004):

$$\frac{\partial C_m}{\partial t} + \mathbf{V} \cdot \nabla C_m = D_m \nabla^2 C_m \tag{2}$$

where C_m is molar concentration, t is time, and D_m is the molecular diffusion coefficient. The boundary condition on the fluid-solid surface is:

$$-\mathbf{n}_{ms} \cdot D_m \nabla C_m = 0 \tag{3}$$

where $\mathbf{n}_{ms}$ is the unit normal pointing from mobile phase to solid.
The intrinsic average concentration is given by

$$\langle C \rangle^m = \frac{1}{V_m} \int_{V_m} C_m dV \tag{4}$$

where $\langle C \rangle^m$ is the intrinsic average concentration of C_m in the mobile phase and V_m is the volume of the mobile phase. We assume near equilibrium conditions at the stationary phase-mobile phase interface. By using the above assumptions and definitions, it can writen (Yan et al., 2010)

$$\frac{\partial \langle C \rangle^m}{\partial t} + \langle \mathbf{v} \rangle^m \cdot \nabla \langle C \rangle^m = \mathbf{D^*} : \nabla \nabla \langle C \rangle^m \tag{5}$$

where $\langle \mathbf{v} \rangle^m$ is the intrinsic local volume average velocity and $\mathbf{D^*}$ is the total dispersion tensor. This makes the longitudinal dispersion coefficient D_{xx} of a given structure as follows

$$\begin{aligned} D_{xx} &= D_m + \frac{D_m}{V_m} \int_{A_{ms}} n_L f_0 \mathrm{d}A - \frac{1}{V_m} \int_{V_m} \left(u - \frac{1}{V_m} \int_{V_m} u \mathrm{d}V \right) f_0 \mathrm{d}V \\ &+ \frac{k}{1+k} \left[\frac{D_m}{V_m} \int_{A_{ms}} n_L f_1 \mathrm{d}A - \frac{1}{V_m} \int_{V_m} \left(u - \frac{1}{V_m} \int_{V_m} u \mathrm{d}V \right) f_1 \mathrm{d}V + \frac{1}{V_m} \int_{V_m} u \mathrm{d}V \frac{1}{A_{ms}} \int_{A_{ms}} f_0 \mathrm{d}A \right] \\ &+ \left(\frac{k}{1+k}\right)^2 \frac{1}{V_m} \int_{V_m} u \mathrm{d}V \frac{1}{A_{ms}} \int_{A_{ms}} f_1 \mathrm{d}A \end{aligned} \tag{6}$$

where k and u are the retention factor and the longitudinal velocity. n_L is the longitudinal component of the unit normal vector **n** pointing from the mobile phase to the particles. A_{ms} is the area of the interface in the cell. f_0 and f_1 are the closure variables (Yan et al., 2010).
The reduced interstitial velocity v_i is defined as

$$v_i = \frac{d_p}{V_m} \int_{V_m} u \mathrm{d}V / D_m \tag{7}$$

where d_p is the pillar diameter. The reduced plate height h represents separation performance of a given structure. In this paper, it has the form

$$h = \frac{2 D_{xx} / D_m}{v_i} \tag{8}$$

The lower reduced plate means better performance. It is independent of the molecular diffusion coefficient and the characteristic dimension. In the numerical simulation, no slip boundary conditions are adopted on the walls, and the periodic boundary conditions are applied for solving the velocity vector and the two closure variables. All the equations are solved with COMSOL™.

3. Model verification

De Smet et al. (2007) computed the reduced plate heights of the channel with different pillar heights. The pillar had a diameter of 5 μm and the sides of the equilateral triangles making up the positioning grid were equal to 6.15 μm. To verify the theoretical model and calculation, we compared the predictions with prior work. We selected the channels with the pillar heights h_p of 5 μm and 12 μm for the verification. We chose water with the density of 1,000 kg/m^3, the dynamic viscosity coefficient of 1.0x10^{-3} Pa•s and the molecular diffusion coefficient of 1.0x10^{-9} m^2/s as working fluid. We give the noslip conditions at the walls of the unit cells. Periodic boundary conditions are adopted for the others. The grid independence of all the computational cases in this paper must be checked for accurate results. By mesh refinement, it should be ensured that the variation between the results is less than 1.0 %. When the maximum element size is 6.0x10^{-7} m for the subdomain, the computational results of two unit cells with different heights are good enough for different interstitial velocities. In the simulation, the total element numbers of the unit cells with the pillar heights of 5 μm and 12 μm are 7,010 and 21,949.
In the range of parameters considered here, the maximum and average deviations with all the given pillar heights are less than 12.5 % and 4.0 %. It can be considered that the results are consistent with the data in De Smet et al.'s paper (2007). The volume-averaging method would be feasible and reliable for investigating the flow characteristics and separation performance of pillar arrays with the staggered arrangement.

4. Results and discussion

Pillar arrays are usually fabricated in the staggered arrangement. According to the volume averaging method, a representative unit cell with appropriate boundary conditions is an available choice. In this paper, we focus on the performance of the 2D structure. Figure 1 shows a representative unit cell used in our calculation. The pillars and channels are shown in gray and white. The pillar has a diameter of 1.00 mm and the sides of the equilateral triangles making up the positioning grid were equal to 1.23 mm. The computational zones for investigating the effect of defects consist of several unit cells in Figure 1.

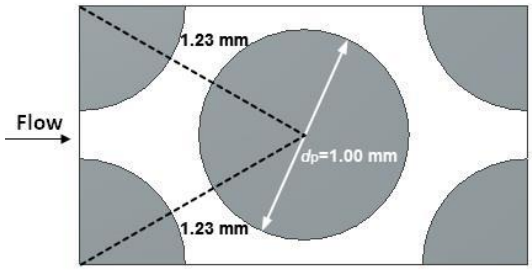

Figure 1: The schematic diagram of a representative unit cell used in our calculation of the pillar array

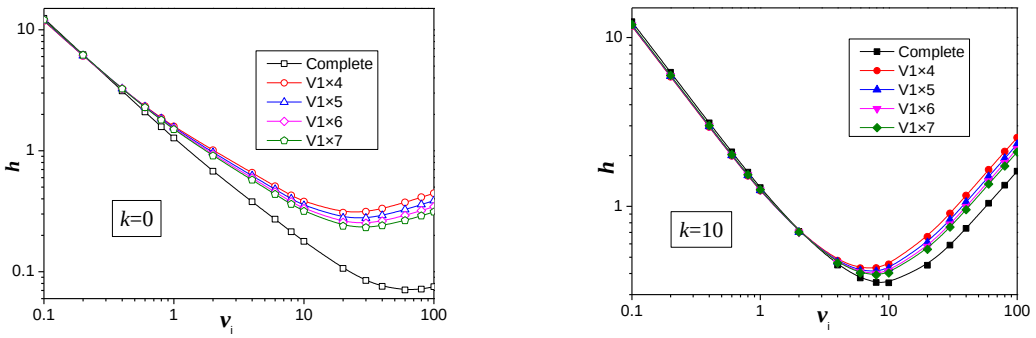

(a) (b)

Figure 2: The reduced plate heights for pillar arrays with complete unit cells and vacancy under (a) nonretentive conditions (k=0) and (b) retentive conditions (k=10)

4.1 The effect of vacancy

In this section, the effects of vacancy on separation performance are examined. In this paper, vacancy is defined as the conditions that one pillar is missing in a given computational zone formed by several unit cells. Figure 2 shows the variations of the reduced plate heights for pillar arrays with the absence of one pillar in one row under nonretentive and retentive conditions. The computational zones in different cases consist of 4 - 7 unit cells in a row. In Figure 2, V1×4, V1×5, V1×6 and V1×7 mean one vacancy in a row with 4, 5, 6 and 7 unit cells. It is found that the reduced plate height of a complete unit cell is the lowest. Moreover, with the increase of the unit cell in a row, the results of the cases with vacancy become smaller gradually. Compared with the results (v_i=100) of a complete unit cell, the reduced plate height of the vacancy case with seven unit cells increases by 317.75 % and 30.00 % under nonretentive and retentive conditions.

In order to give further details and more explanation about the effect of vacancy, more cases are investigated. When the computational zones consist of a row with several unit cells, the vacancy rate is high. Therefore, we considered the cases with multi-row and multi-column unit cells to obtain the effect of lower vacancy rate. V4×4, V6×6, V8×8 and V10×10 mean one vacancy in 4, 6, 8 and 10 rows and columns with the same unit cell. As can be seen in Figure 3, the results between a complete unit cell and the cases with multi-row and multi-column unit cells still have obvious differences. Compared with the results (v_i = 100) of a complete unit cell, the reduced plate height of the vacancy case with ten rows and ten columns (the vacancy rate = 0.5 %) increases by 28.13 % and 7.07 % under nonretentive and retentive conditions. If we want to obtain better performance, the vacancy rate should be within a very small value.

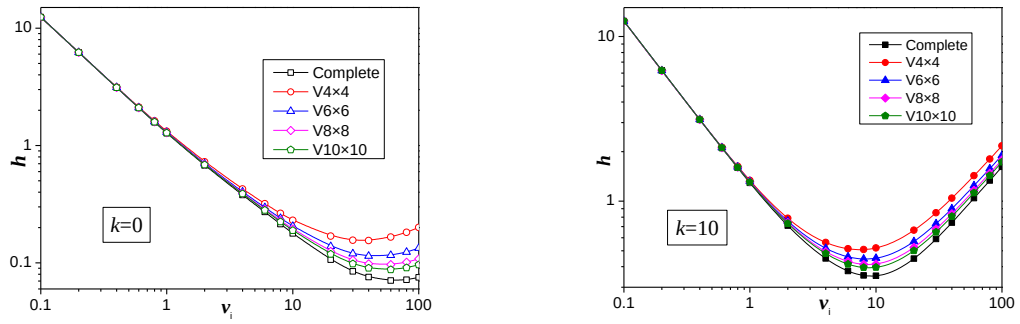

(a) (b)

Figure 3: The reduced plate heights for pillar arrays with complete unit cells and vacancy under (a) nonretentive conditions (k=0) and (b) retentive conditions (k=10)

4.2 The effect of damage

In this section, the effect of damage on the reduced plate height is discussed, and the computational zones consist of four unit cells in a row. In the paper, damage means the cases with different arch heights of the missing part. First, the effect of the damage position is investigated. The position of the missing part in the flow field is shown in Figure 4. The arch height of the missing part is 0.1d_p. In Figure 5 and 6, D1/10, D3/10, D5/10, D7/10 and D9/10 mean that the arch heights of the missing part are 0.1d_p, 0.3d_p, 0.5d_p, 0.7d_p and 0.9d_p. a, b, c and d represent the spatial relationship between the damaged pillar and flow direction, as shown in Figure 4.

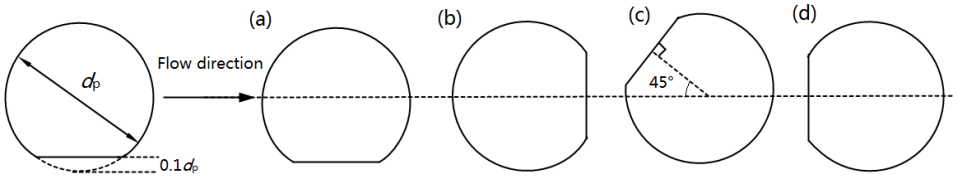

Figure 4: Schematic description of the spatial relationship between the damaged pillar and flow direction

Figure 5 shows the variations of the reduced plate heights for pillar arrays with different damage positions under nonretentive and retentive conditions. As revealed by the graph, no significant changes are found in the

influence of damage positions on the reduced plate height when the damage part is small. In the staggered arrangement, the influence of damage positions can be reduced or even eliminated to some extent.

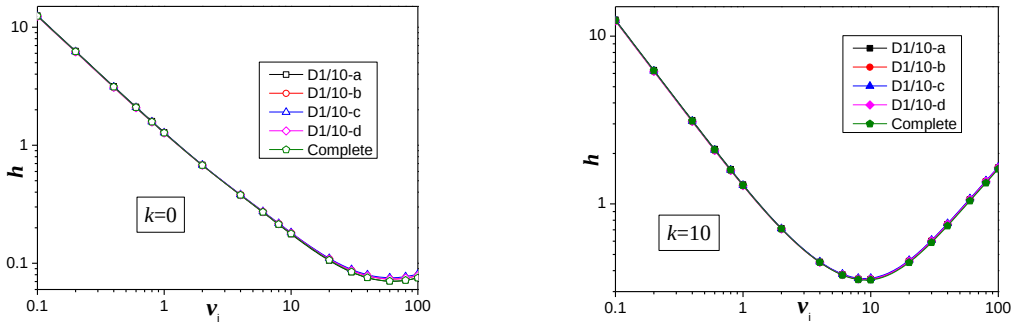

(a) (b)

Figure 5: The reduced plate heights for pillar arrays with complete unit cells and one damaged pillar under (a) nonretentive conditions (k=0) and (b) retentive conditions (k=10)

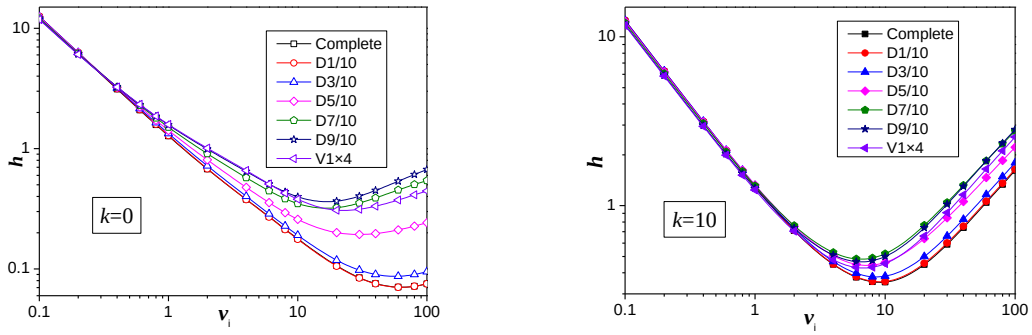

(a) (b)

Figure 6: The reduced plate heights for pillar arrays with complete unit cells and one damaged pillar under (a) nonretentive conditions (k=0) and (b) retentive conditions (k=10)

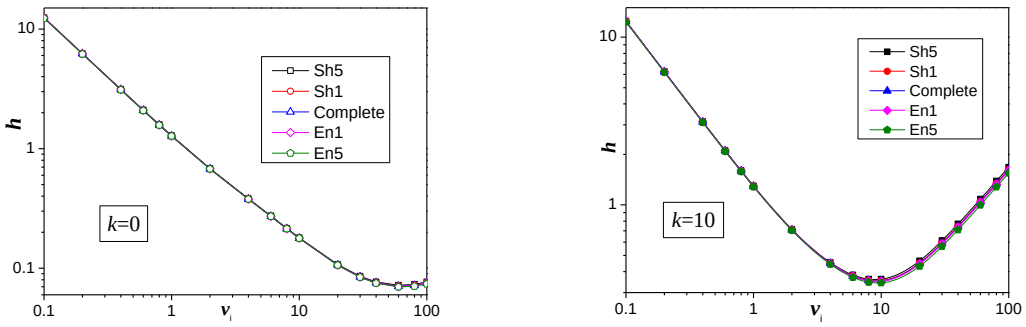

(a) (b)

Figure 7: The reduced plate heights for pillar arrays with complete unit cells and one fabrication inaccurate pillar under (a) nonretentive conditions (k=0) and (b) retentive conditions (k=10)

For further study, the size of the missing part is considered as an important parameter. The arch heights of the missing parts in the computational zones are from $0.1d_p$ to $0.9d_p$. Figure 6 shows the reduced plate heights for

pillar arrays with different arch heights of the missing parts. It is found that the significant increase of the reduced plate height appears when the arch height of the missing part is more than 0.3 d_p. The results of the case with vacancy are superior to those of D7/10 and D9/10. A possible explanation for this is that badly damaged pillars impede longitudinal flow. Compared with the results (v_i = 100) of a complete unit cell, the reduced plate height of D9/10 increases by 789.32 % and 74.97 % under nonretentive and retentive conditions.

4.3 The effect of fabrication inaccuracy

In this section, the computational zones consist of four unit cells in a row. In order to investigate the effect of fabrication inaccuracy, one pillar in the computational zones are shrunk or enlarged and the others remain the original diameter. Sh1 and Sh5 mean the computational zone with one pillar shrunken by 0.01d_p and 0.05d_p, . En1 and En5 represent the computational zone with one pillar enlarged by 0.01d_p and 0.05d_p. Figure 7 shows that the reduced plate heights for pillar arrays with one fabrication inaccurate pillar. In the first and second case, one pillar in computational zones is shrunk by 0.05d_p and 0.01d_p. In the third and fourth case, one pillar in computational zones is enlarged by 0.01d_p and 0.05d_p. As can be seen in Figure 8, the results between the cases with one fabrication inaccurate pillar have no significant difference. Compared with the results of a complete unit cell, all the average deviations are less than 2.3 %.

5. Conclusions

In this paper, we have studied the effect of vacancy, damage and dimensional accuracy on separation performance by the method of volume averaging. Vacancy has remarkable influence on separation performance. Even though the vacancy rate is very low, the influence cannot be neglected. When the size of the missing part is greater than 0.3d_p, the differences can be observed. Serious damage can lead to lower performance of the system than that of the case with vacancy. The effect of fabrication inaccuracy on the reduced plate height is not obvious in the range of our study. Therefore, it is advisable to pay due attention to vacancy and serious damage in industrial production.

Acknowledgments

We would like to acknowledge financial supports for this work provided by National Natural Science Foundation of China (No. 51536007, 51476124).

References

Buyuktas D., Wallender W.W., 2004, Dispersion in Spatially Periodic Porous Media, Heat and Mass Transfer, 40(3-4), 261-270.

De Smet J., Gzil P., Baron G.V., Desmet G., 2007, On the 3-dimensional Effects in Etched Chips for High Performance Liquid Chromatography Separations, Journal of Chromatography A, 1154(Compendex), 189-197.

Fee C., Nawada S., Dimartino S., 2014, 3D Printed Porous Media Columns with Fine Control of Column Packing Morphology, Journal of Chromatography A, 1333, 18–24.

Rahim N.A.A., Azudin N.Y., Shukor S.R.A., 2017, Computational Fluid Dynamic Simulation of Mixing in Circular Cross Sectional Microchannel, Chemical Engineering Transactions, 56, 79-84.

Santana H.S., Amaral R.L., Taranto O.P., 2015, Numerical Study of Mixing and Reaction for Biodiesel Production in Spiral Microchannel, Chemical Engineering Transactions, 43, 1663-1668.

Seeger K., Palmer R.E., 1999, Fabrication of Ordered Arrays of Silicon Nanopillars, Journal of Physics D: Applied Physics, 32(24), 129–132.

Sinitskii A., Neumeier S., Nelles J., Fischer M., Simon U., 2007, Ordered Arrays of Silicon Pillars with Controlled Height and Aspect Ratio, Nanotechnology, 18, 1–6.

Wang D., Ji R., Du S., Albrecht A., Schaaf P., 2013, Ordered Arrays of Nanoporous Silicon Nanopillars and Silicon Nanopillars with Nanoporous Shells, Nanoscale Research Letters, 8, 1–9.

Yan X.H., Wang Q.W., Bau H.H., 2010, Dispersion in Retentive Pillar Array Columns, Journal of Chromatography A, 1217(8), 1332-1342.

Yan X.H., Liu M., Zhang J.K., Zhu H.R., Li Y.F., Liang K., 2015, On-chip Investigation of the Hydrodynamic Dispersion in Rectangular Microchannels, Microfluidics and Nanofluidics, 19(2SI), 435-445.

Zhu T.T., Zhao Y.H., Diao Y.H, Li F.F., Quan Z.H., 2017, Experimental Investigation and Performance Evaluation of a Vacuum Tube Solar Air Collector Based on Micro Heat Pipe Arrays, Journal of Cleaner Production, 142, 3517-3526.